NEUROSCIENCE
RESEARCH ARTICLE
K. Horie et al. / Neuroscience 448 (2020) 312–324

Investigation of *Oxtr*-expressing Neurons Projecting to Nucleus Accumbens using *Oxtr-ires-Cre* Knock-in prairie Voles (*Microtus ochrogaster*)

Kengo Horie, [a,b] **Kiyoshi Inoue,** [b] **Katsuhiko Nishimori** [a*†] **and Larry J. Young** [b,c*†]

[a] *Laboratory of Molecular Biology, Department of Molecular and Cell Biology, Graduate School of Agricultural Science, Tohoku University, 468-1, Aramaki Aza-Aoba, Aoba-ku, Sendai, Miyagi 980-0845, Japan*

[b] *Silvio O. Conte Center for Oxytocin and Social Cognition, Center for Translational Social Neuroscience, Yerkes National Primate Research Center, Emory University, 954 Gatewood Road, Atlanta, GA 30329, USA*

[c] *Department of Psychiatry and Behavioral Sciences, Emory University School of Medicine, 954 Gatewood Road, Atlanta, GA 30329, USA*

Abstract—Social bonds such as parent–infant attachment or pair bonds can be critical for mental and physical well-being. The monogamous prairie vole (*Microtus ochrogaster*) has proven useful for examining the neural substrates regulating social behaviors, including social bonding. Oxytocin (OXT) and oxytocin receptor (OXTR) play critical roles in alloparental care, pair bonding and consoling behavior in prairie voles. While OXTR in a few regions, such as the nucleus accumbnes (NAcc), prefrontal cortex (PFC) and anterior cingulate cortex (ACC), have been implicated in regulating these behaviors, the extent to which other OXT sensitive areas modulate social behaviors has not been investigated. The NAcc is a central hub for modulating OXTR dependent social behaviors. To identify neurons expressing *Oxtr* in prairie vole brain, we generated gene knock-in voles expressing *Cre recombinase* in tandem with *Oxtr* (*Oxtr-ires-Cre*) using CRISPR/Cas9 genome editing. We confirmed *Oxtr* and *Cre* mRNA co-localization in NAcc, validating this model. Next, we identified putative *Oxtr*-expressing neurons projecting to NAcc by infusing retrograde CRE-dependent EGFP AAV into NAcc and visualizing fluorescence. We found enhanced green fluorescent protein (EGFP) positive neurons in anterior olfactory nucleus, PFC, ACC, insular cortex (IC), paraventricular thalamus (PVT), basolateral amygdala (BLA), and posteromedial and posterolateral cortical amygdaloid area (PMCo, PLCo). The ACC to NAcc OXTR projection may represent a species-specific circuit since *Oxtr*-expressing neurons in the ACC of mice were reported not to project to the NAcc. This is the first delineation of *Oxtr*-expressing neural circuits in the prairie vole, and demonstrates the utility of this novel genetically modified organism for characterizing OXTR circuits involved in social behaviors.

Key words: oxytocin receptor, genome editing, nucleus accumbens, social bonding, neural circuits, CRISPR.

INTRODUCTION

Social bonds such as the close and enduring attachments between parents and infants or between opposite sex mates in monogamous mammals can play a critical role in promoting mental and physical well-being (Feldman, 2012). Disruption of social bonds can have devastating effects on mental and physical health (Bosch and Young, 2018; Pohl et al., 2019). Recent research has focused on understanding how genes, neuronal modulators, receptors, and circuits regulate social bond formation and maintenance, which may have translational implications for improving quality of life in certain psychiatric disorders such as autism, PTSD, and depression (Modi et al., 2015; Arai et al., 2016; Bosch et al., 2016; King et al., 2016; Amadei et al., 2017; Hirota et al., 2020).

*Corresponding authors. Address: Dept. of Obesity and Internal Inflammation, Fukushima Medical University, Hikarigaoka 1, Fukushima City, Fukushima Pref. 960-1295, Japan (K. Nishimori). Yerkes National Primate Research Center, 954 Gatewood Road, Atlanta, GA 30329, USA (L. J. Young).
E-mail addresses: knishimo@fmu.ac.jp (K. Nishimori), lyoun03@emory.edu (L. J. Young).
† These authors equally contributed to this work as corresponding authors.

Abbreviations: ACC, anterior cingulate cortex; AON, anterior olfactory nucleus; BLA, basolateral amygdala; CeA, central amygdala; CoA, cortical amygdala; EGFP, enhanced green fluorescent protein; IC, insular cortex; NAcc, nucleus accumbnes; OXT, oxytocin; OXTR, oxytocin receptor; *Oxtr-ires-Cre*, *Cre recombinase* in tandem with *Oxtr*; PFC, prefrontal cortex; PrL, prelimbic cortex; PVT, paraventricular thalamus; VTA, ventral tegmental area; PMCo, posteromedial cortical amygdala; PLCo, posterolateral cortical amygdala.

https://doi.org/10.1016/j.neuroscience.2020.08.023
0306-4522/

The prairie vole (*Microtus ochrogaster*) is a monogamous rodent species showing enduring pair bonding between mates, biparental care, and the consoling behavior toward a distressed partner (Young and Wang, 2004; Aragona et al., 2006; Gobrogge et al., 2009; Young et al., 2011; Johnson and Young, 2015; Burkett et al., 2016; Walum and Young, 2018). Prairie voles have proven to be an ideal model for investigating brain mechanisms that regulate social bonding though studying the pair bond (McGraw and Young, 2010; Walum and Young, 2018). Oxytocin (OXT) and oxytocin receptor (OXTR) are one of the key neuromodulators and receptors mediating pair bond formation and maintenance in prairie voles (Donaldson and Young, 2008; Smith and Wang, 2014; Barrett et al., 2015; Bosch, et al., 2016; Johnson et al., 2016, 2017; Walum and Young, 2018). OXT is produced in neurons in the paraventricular nucleus (PVN) and supraoptic nucleus of the hypothalamus and their projections course throughout the forebrain (Ross et al., 2009; Johnson and Young, 2017; Rogers et al., 2018). OXT binds to OXTR, which is a G protein coupled receptor coupling with $G\alpha_{q/11}$ and transducing intracellular signaling (Jurek and Neumann, 2018). OXT/OXTR signaling acts as a neuromodulator affecting social and sexual behavior, stress coping, and the processing of social stimuli, in many species (Knobloch et al., 2012; Dolen et al., 2013; Choe et al., 2015; Marlin et al., 2015; Wei et al., 2015; Oettl et al., 2016; Yokoi et al., 2020). It has been proposed that OXT acts in multiple brain regions to enhance the neural processing of social signals, increase the salience and reinforcing value of social cues, and facilitate the formation of social memories, processes critical for social bond formation. OXTR signaling in the nucleus accumbens (NAcc) plays a particularly important role in pair bond formation and maintenance in prairie voles (Young et al., 2001; Keebaugh et al., 2015). However, it is increasingly clear that OXTR signaling in a distributed social salience network is critical for many aspects of social cognition involved in pair bonding, and the NAcc is a central hub of that network (Johnson, et al., 2017). Indeed OXTR signaling appears to coordinate neural activity across the social salience network during mating (Johnson, et al., 2016) which is hypothesized to facilitate the flow of social information across the network, ultimately leading to synaptic plasticity in the NAc that enhances the reinforcing value of the partner's cues (Walum and Young, 2018). However, the extent to which OXTR expressing neurons in regions of the social salience network, such as the anterior olfactory nucleus, prefrontal cortex (PFC), anterior cingulate cortex (ACC), and basolateral amygdala (BLA) directly project to the NAcc is unknown. Although some circuits projecting to NAcc are known to regulate reward processing in rodents (Zhu et al., 2016; Otis et al., 2019; Lafferty et al., 2020), only a few studies have explored the function and anatomy of these circuits in prairie voles (Amadei, et al., 2017) and the relationships between these circuits and the OXT/OXTR system remains to be elucidated. To begin to explore the interconnected nature of OXTR circuits with the NAcc that may be involved in social bonding in prairie voles, we generated *Oxtr-internal ribosomal entry site (ires)-Cre* prairie voles using clustered regularly interspaced short palindromic repeat (CRISPR)/CRISPR associated protein (Cas) genome editing.

Adeno associated virus (AAV) has been proven useful as a tracer to visualize afferent and efferent neuronal circuits in rodents (Chamberlin et al., 1998; Tervo et al., 2016). Anterograde AAV carrying fluorescent proteins like enhanced green fluorescent protein (EGFP) can be expressed in cell bodies of neurons exclusively, and by tracing fibers filled with EGFP in the whole brain, efferent projections can be determined (Bosch et al., 2016). Retrograde AAV can transduce axon terminals in the injection site, be transported to the cell body, and express in neurons that project to injection site and afferent projections of the injection site can be determined. To our knowledge, retrograde AAV tracing studies have yet to be used in prairie voles to identify cell-type specific afferent projections in prairie voles.

Although the expression of *Oxtr* in brains of prairie voles has shown by autoradiography (Witt et al., 1991; Insel and Shapiro, 1992), it has not been possible to visualize *Oxtr* expressing neurons at a cellular level, or examine their projections in prairie voles. To examine neural circuits expressing *Oxtr* that project to NAcc specifically, a knock-in prairie vole that expresses *Cre recombinase* (*Cre*) under the control of *Oxtr* would be useful, however embryonic stem cells- or induced pluripotent stem cells-based homologous recombination has not been achieved in prairie voles. Alternatively, the CRISPR/Cas9 system has been proven to be useful for generating gene knock in animals because double strand break, generated by site-specific endonuclease-like activity by CRISPR/Cas9, stimulates and accelerate homologous recombination (Aida et al., 2015; Boender and Young, 2020). The CRISPR/Cas system is an RNA-based adaptive immune system of archaea and bacteria against bacteriophage or foreign nucleic acids (Barrangou et al., 2007; Wiedenheft et al., 2012). CRISPR/Cas9 system derived from Streptococcus pyogenes is in the Type II – A CRISPR/Cas system consisting of Cas9 nuclease and two short RNAs, crispr RNA (crRNA) and trans activating crRNA (tracrRNA) (Deltcheva et al., 2011). crRNA containing 20 nt of sequence homologous with the target genome, tracrRNA, and Cas9 protein bind to the target region adjacent to the 5′-NGG-3′ palindromic adjacent motif (PAM) sequence. Cas9 induces a double strand break into the target sequence and insertions or deletions are induced into the target sequence while it is repaired by endogenous DNA repair pathways (Cho et al., 2013; Cong et al., 2013; Mali et al., 2013; Wang et al., 2013). At that time, if there are homologous templates like knock-in plasmids or single strand DNAs, and exogenous DNA sequence can be inserted in the targeted region (Wang, et al., 2013; Aida, et al., 2015; Boender and Young, 2020).

In this study, we first generated a knock-in prairie vole carrying *ires – Cre* in the *Oxtr* gene by using CRISPR/Cas9. This is the first reported knock-in prairie vole, demonstrating the potential of this strategy for diversifying the genetic tools available for this model

organism. By combining the *Oxtr-ires-Cre* knock-in prairie vole with the injection of retrograde AAV carrying CRE-dependent EGFP, we mapped the *Oxtr*-expressing neurons that project to NAcc (afferents) and report evidence that prairie voles may have novel OXT sensitive circuits relevant to their species-specific social behavioral repertoire.

EXPERIMENTAL PROCEDURES

Animals

Prairie vole colonies were maintained first at Tohoku University in Japan and then at Emory University in Atlanta as described previously (Horie et al., 2019). The Tohoku colony originated from the Emory University colony, which were originally derived from field caught specimens from Illinois, USA. Opposite sex pairs were housed together to breed. After weaning at postnatal day (P) 20–23, the offspring were separated from their parents and housed in groups of up to three same-sex siblings per cage. All animals were housed using alternating 12-h periods of light and dark at 25 °C and were allowed *ad libitum* access to food (Labo MR Stock, NOSAN, Japan, or Laboratory Rabbit Diet HF 5326, LabDiet) and water. All animal experiments were performed according to a protocol approved by Tohoku University Guidelines for Animal Experimentation or by the Institutional Animal Care and Use Committee at Emory University.

Construction of crRNA and the knock-in plasmid

The crRNA targeting the 3′ untranslated region (UTR) of the prairie vole *Oxtr* was designed using Benchling (https://www.benchling.com). The crRNA with the desired spacer sequence (5′ – TTCAGCATGAGCCACCTGTCTGG – 3′) and tracrRNA were synthesized by GenomeCraft service of FASMAC (GE-001, FASMAC, Japan). The efficiency of the crRNA was confirmed by *in vitro* digestion assay (IDA) as described previously (Aida et al., 2015) (Supplementary Fig. 1).

A knock-in plasmid containing *ires-Cre* sequence flanked by homology arms were made with In-Fusion HD Cloning kit (638909, Clontech, Japan). *Ires-Cre* sequence was placed 7 bp downstream from the stop codon of *Oxtr* gene. Seven hundred fifty base pairs of 5′ and 3′ homology arms were amplified with a forward primer 5′ – CCGCGGGAATTCGATCAGGCAGG TTGGAAGTTG – 3′ and a reverse primer 5′ – CGCGGTGGGCCAGACAGGTGGCTCATGCTGAAG – 3′, and a forward primer 5′ – GTCTGGCCCACCG CGCCT – 3′ and a reverse primer 5′ – GAATTCACTAGT GATCAGCTCCAGAGTGTGTGT – 3′ respectively. The pGEM-T-easy vector (Promega, Madison WI, USA) was linearized by PCR with a forward primer 5′ – ATCAC TAGTGAATTCGCGGC – 3′ and 5′ – ATCGAATTC CCGCGGCCGCC – 3′ and homology arms were cloned into linearized pGEM T-easy vector with In-Fusion HD Cloning kit (638909, Clontech, Japan) (pGEM-arm). The *Ires-Cre* sequence was amplified from the genome of *Oxtr-ires-Cre* knock-in mouse (Hidema et al., 2016) by PCR with a forward primer 5′ – CAGCATGA GCCACCTAGATGGGGGTCCTGGGCC – 3′ and a reverse primer 5′ – CGCGGTGGGCCAGACCTA ATCGCCATCTTCCAGC – 3′ and cloned into pGEM-arm linearized by PCR with a forward primer 5′ – GTCTGGCCCACCGCGCCTGC – 3′ and 5′ – AGGTGGCTCATGCTGAAGAT – 3′. Every PCR was performed with PrimeSTAR GXL DNA Polymerase (R050B, Takara, Japan) and T100 thermal cycler (Promega, Madison WI, USA).

Embryo manipulations

Superovulation and embryo collection. Superovulation and embryo transfer were performed as described previously (Horie et al., 2015, 2019). Briefly, 48 h after 60 IU pregnant mare serum gonadotropin was administered to the female prairie vole, 60 IU human chorionic gonadotropin was administered and the subject was allowed to mate with the stud male for 16 h. Then embryos were collected from oviducts of the female and cultured in G-1 PLUS medium (10128, Vitrolife, Sweden) at 37 °C with 5 % CO_2 until they were used for the microinjection.

Microinjection of crRNA, tracrRAN, and Cas9 protein

Microinjecting Cas9 nuclease protein, synthetic crRNA, and tracrRNA to the nucleus and cytoplasm of embryos instead of microinjecting Cas9 mRNA and single guide RNA dramatically improved knock-in efficiency in mouse (Aida et al., 2015). Thus, we used this strategy to generate *Oxtr-ires-Cre* knock-in prairie voles.

Thirty ng/μl Cas9 nuclease protein (M0386S, NEB, Ipswich, MA USA), 0.61 pmol/μl crRNA, 0.61 pmol/μl tracrRNA, and 10 ng/μl knock-in plasmid were prepared in Nuclease-Free water (AM9932, Ambion, Austin TX, USA). The mixture was injected into the nucleus and cytoplasm of embryos with a microinjector (IM-11-2, Narashige, Japan) and a micromanipulator (MN-4,M0-202U, Narashige, Japan) under an inverted microscope (Ts2R, Nikon, Japan). Injected embryos were cultured in G-1 Plus medium for 16–20 h until they developed to the 2-cell stage.

Embryo transfer

Injected embryos were transferred to the oviducts of pseudopregnant female voles as described previously (Horie et al., 2019). Briefly, up to 15 injected embryos were transferred into the oviducts of pseudopregnant female voles with a glass capillary. Twenty days later, the subjects gave birth pups.

Genotyping and Sanger sequencing of *Oxtr* in newborns

Tissues were collected from their ear punches or toe clips and the target regions were amplified with three primer pairs (5′ arm PCR, F1 and R1, 5′ – GCCAGGCA GAGAGTTTTGTC – 3′ and 5′ – CAGAGCAGCCCTG TACATCA – 3′; insert PCR, F2 and R2, 5′ –

ATGGTCCCAGAGTGACCCTTTG – 3′ and 5′ – TTGTCCTAGCCCACTGGGTTTC – 3′; 3′ arm PCR, F3 and R3, 5′ – TGGAAGATGGCGATTAGGTC – 3′ and 5′ – CGAGGTTACAAACGCACTGA – 3′) and analyzed by gel electrophoresis as shown in Fig. 1. Each PCR amplicon from cre1 vole was purified and cloned into pGEM-T easy vector, and 10 of each plasmid were sequenced using Sanger sequencing.

Off target analysis

Potential off-target sequences were predicted by Benchling. The off-target site having the score higher than 0.8 was regarded as a potential off-target site and nine potential off-target sites were detected. Each potential off-target was amplified from genomes of 14 voles that were the breeding pairs of F3 generation by PCR with each primer set (OffT1: 5′ – CTTAC CAGATGGTCAACAGC – 3′ and 5′ – TCTAGGAC AGTGATCTTGCC – 3′; OffT2: 5′ – TTATGTCTGTGT ACTACCTA – 3′ and 5′ – TACATATATAGACATAGTTA – 3′, or 5′ – GAGGCTCAGTGCCCACACCT – 3′ and 5′ – AAGTGGCTCATACCTACCTG – 3′; OffT3: 5′ – ATTC ACGGTTATATGGGCAT – 3′ and 5′ – TCTC AATAAAATAACAAGGG – 3′; OffT4: 5′ – TCACACTT GGGGATTCTGTG – 3′ and 5′ – TTTGCACAA TAAAGGGGATC – 3′; OffT5: 5′ – AGGGCCCTGC ACACAGTGAC – 3′ and 5′ – GTATGTCAGTGCA TGCATGT – 3′; OffT6: 5′ – TAGAATTTTGTCTGG AAGTT – 3′ and 5′ – AATACAAGTAAAATATCACT – 3′; OffT7: 5′ – GAATTGGCAATGTTGTTGCT – 3′ and 5′ – ACTTATCCTCAACCACTGCC – 3′; OffT8: 5′ – GCCT GCCTTTGCTTCTCAGG – 3′ and 5′ – AGACAGT AAAGGGAATAATG – 3′; OffT9: 5′ – TGGAAAC TTTAAACTCTGCA – 3′ and 5′ – TTTTGCAGAGCT GTAAGAGT – 3′) and directly sequenced by the sanger sequencing with each sequencing primer (OffT1: 5′ – CTTACCAGATGGTCAACAGC – 3′ or 5′ – AACACAGG CTCTTTAAGTCC – 3′; OffT2: 5′ – GTCTGTGTAC TACCTATGTA – 3′ or 5′ – ACACAGTACCCGGA GACTCCAG – 3′; OffT3: 5′ – ATTCACGGTTATATGGG CAT – 3′; OffT4: 5′ – TCACACTTGGGGATTCTGTG – 3′; OffT5: 5′ – AGGGCCCTGCACACAGTGAC – 3′; OffT6; 5′ – TAGAATTTTGTCTGGAAGTT – 3′; OffT7; 5′ – GAATTGGCAATGTTGTTGCT – 3′, 5′ – CATCTTCAT TTCTGACTCAT – 3′, 5′ – ACTTATCCTCAACC ACTGCC – 3′, or 5′ – CCTCAACCACTGCCTTCCCG – 3′; OffT8: 5′ – GCCTGCCTTTGCTTCTCAGG – 3′, or 5′ – CTTAACTATCTGGGCCACCG – 3′; OffT9: 5′ – TGGAAACTTTAAACTCTGCA – 3′).

RNAscope *in situ* hybridization (ISH)

Prairie voles were deeply anesthetized by Isoflurane and euthanized by decapitation and their brains were immediately removed and frozen on dry ice and stored at −80 °C until they were sliced. Twenty μm thick brain slices were prepared on a cryostat (CryoStar™ NX-70, ThermoFisher Scientific, USA).

A prairie vole specific *Oxtr* probe (422561-C3, Advanced Cell Diagnostics, Inc, USA) and a *Cre* probe (312281-C2, Advanced Cell Diagnostics, Inc, USA) were used for fluorescent RNAscope ISH. Brain slices mounted on the glass slides (Superfrost Plus Microscope Slides, Fisherbrand, USA) were placed in 4% paraformaldehyde (PFA) for 15 min at 4 °C. Slices were dehydrated serially in 50% ethanol for 5 min, 70% ethanol for 5 min, and 100% ethanol for 5 min at room temperature, and then incubated in 100% ethanol at −20 °C over a night. Slides were dried for 5 min and barriers were drawn with an Immedge™ hydrophobic barrier pen (H-4000, Vector Laboratory, USA) around each section. Protease IV (Advanced Cell Diagnostics, Inc, USA) was applied and slides were incubated for 30 min at room temperature followed by two washes in PBS. *Oxtr* and *Cre* probes were diluted in C1 probe diluent (Advanced Cell Diagnostics, Inc, USA) in 3:1:100 ratios, respectively. The mixture was applied to slides and incubated for 2 h at 40 °C. Slides were washed in 1× wash buffer (Advanced Cell Diagnostics, Inc, USA) twice for 2 min each at room temperature and Amp 1-FL was put on the sections and the slides were incubated for 30 min at 40 °C. The slides were then washed in 1× wash buffer for 2 min at room temperature twice and Amp 2-FL was applied to the sections and they were incubated for 15 min at 40 °C. The slides were then washed in 1× wash buffer for 2 min at room temperature twice and Amp 3-FL was applied to the sections and they are incubated for 30 min at 40 °C. Slides were then washed in 1× wash buffer for 2 min at room temperature twice and Amp 4-FL was applied to the sections and they are incubated for 15 min at 40 °C. Slides were washed in 1× wash buffer for 2 min at room temperature twice, and then DAPI (Advanced Cell Diagnostics, Inc, USA) was applied to the sections and incubated for 30 s at room temperature. Excess liquid was removed and ProLong Gold Antifade Mountant (P36930, Thermo Fisher Scientific, USA) was applied onto each section and cover slips were placed on slides.

Images were taken using the Keyence microscope (BZ-X700, Keyence, Japan) with ×40 lens.

OXTR receptor autoradiography

Brain sections were prepared according to the methods described in the RNAscope ISH section. OXTR autoradiography was performed as described previously (Horie et al., 2019).

Colony maintenance and genotyping

For daily genotyping, a primer pair of 5′ – AAATGCTTCTGTCCGTTTGC – 3′, 5′ – TGCCTTCATCATCGCCATGC – 3′, and 5′ – GAGCACTCAGGTTGGGGTAG – 3′ were used for PCR. It is performed using KAPA2G Robust PCR Kits, HotStart ReadyMix (KK5701, Roche, Switzerland) with touchdown PCR. PCR mixtures were denatured at 94 °C for 3 min, then denatured at 94 °C for 10 s. They were annealed with primers at 65 °C for 30 s, and extendedat 68 °C for 1 min, and then, this cycle was repeated ten times with decreasing annealing temperature 0.5 °C per cycle. Then 28 cycles of denature at 94 °C for 10 s, annealing at 60 °C for 30 s,

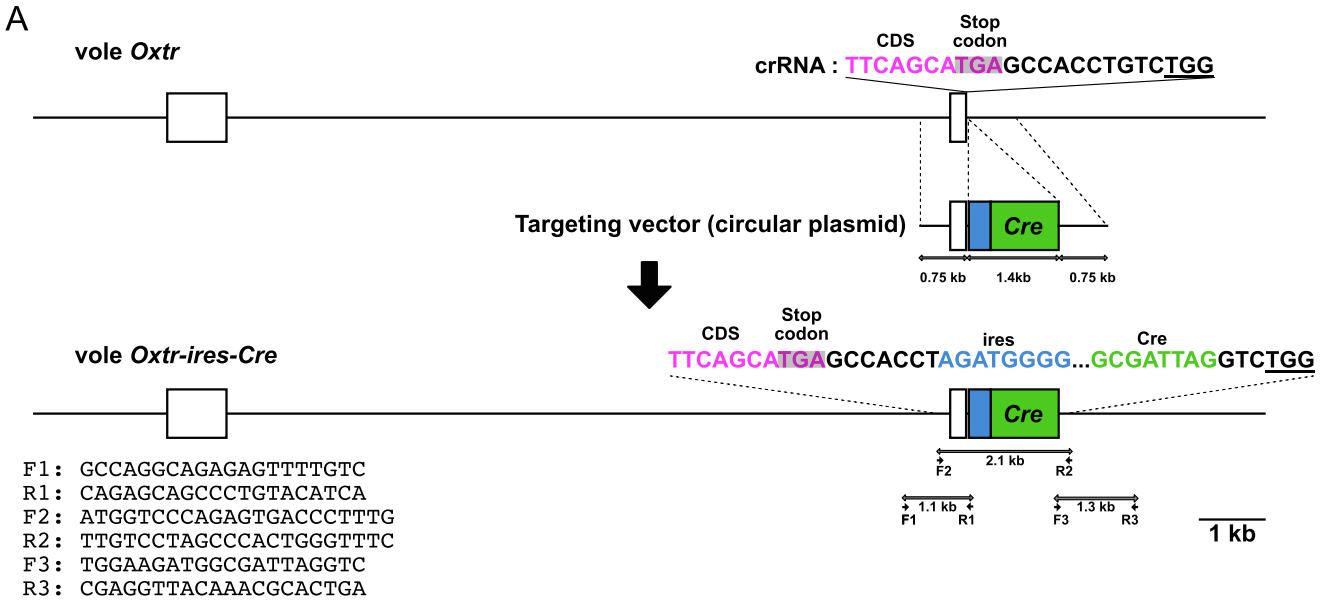

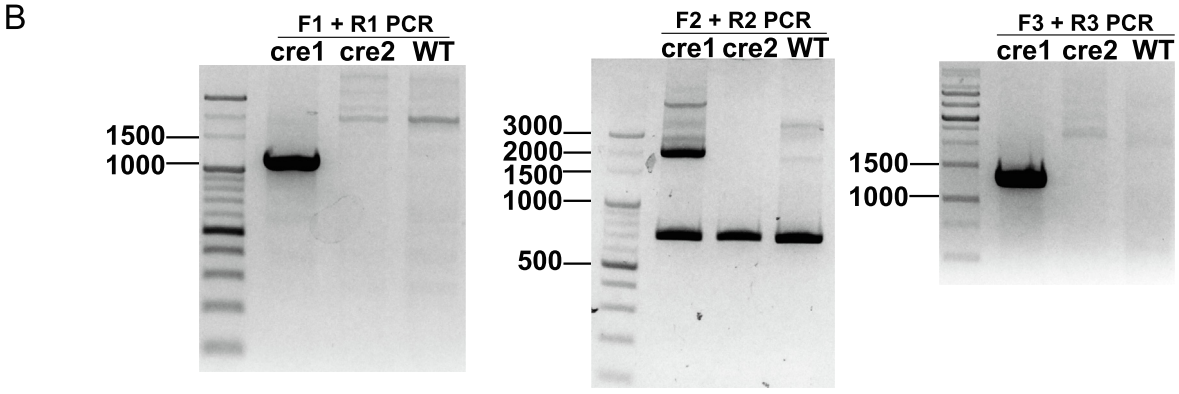

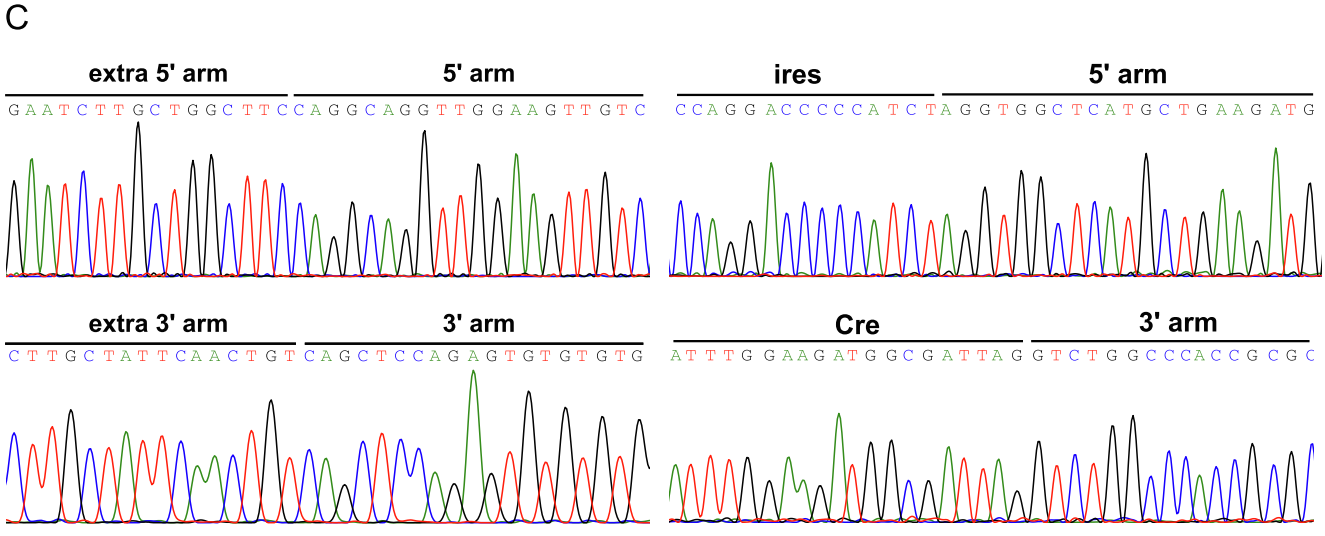

Fig. 1. Generation of *Oxtr-ires-Cre* knock-in prairie voles. **(A)** The *Oxtr* gene was targeted by a crRNA targeting TTCAGCATGAGCCACCTGTC. The underline indicates the PAM sequence. The ires-Cre sequence was placed at the 7 bp downstream from the stop codon of *Oxtr*. Coding sequence (CDS), magenta; ires, blue; Cre, green; stop codon, gray highlight. **(B)** Cre1 was confirmed as a knock-in vole by the PCR analysis. **(C)** The target region of Cre1 was sequenced and confirmed as a knock-in vole. The boundary sequences between endogenous sequences and knock-in arms, and arms and *ires-Cre* sequence were shown as representative figures to show the precise knock-in.

and extension at 72 °C for 1 min were performed and amplicons were analyzed by the gel electrophoresis in 2% Agarose gel.

Stereotaxic injection

Subjects were anesthetized with 3% Isoflurane and anesthesia was maintained with 1–3% Isoflurane during surgery. They were administered with 2 mg/kg Meloxicam as a pre-surgical analgesic. The head was fixed with ear bars coated with Lidocaine and a small incision was made on the head. To visualize projections of *Oxtr*-expressing neurons to NAcc, 200–1000 nl of AAVrg- the human synapsin promoter (hSyn)-DIO-EGFP (7.6×10^{12} gc/ml, 50457-AAVrg, Addgene, USA) was injected into NAcc (anteroposterior: +1.7 mm; mediolateral: 0.85 mm; dorsoventral; 5.00 mm) with a NanoFil syringe (NanoFil, World Precision Instruments, USA) with the NanoFil needle (NF33BL-2, World Precision Instruments, USA) at 100 nl/min by using Micro 4 microinfusion pump (World Precision Instruments, USA). Subjects were administered 2 mg/kg Meloxicam on the following day and recovered for 2 weeks.

Immunostaining and imaging

Subjects injected with AAVrg-hSyn-DIO-EGFP were perfused with 4% PFA and brains were removed from their skulls. Brains were incubated in 4% PFA for 16 h and then placed in 2% Agarose in PBS. Fifty μm thick slices were prepared for using a vibratome (VT1200, Leica, USA) and served for immunohistochemistry.

Sections were washed in PBS three times at room temperature. They were incubated in 0.05% Triton X-100 in PBS (PBST) for 30 min for penetrating and then incubated in 5% normal horse serum (16050122, Thermo Fisher Scientific) in PBST (NPBST) for 30 min for blocking. Sections were incubated with rabbit anti-GFP antibody (598, MBL, Japan) diluted 1/1000 in NPBST for 16 h at 4 °C. Then, the sections were washed in PBS three times at room temperature and incubated with goat anti-rabbit IgG secondary antibody conjugated with Alexa Fluor 488 diluted 1/400 in NPBST (A-11008, Thermo Fisher Scientific) with DAPI diluted 1/1000 for 1 h at room temperature. Sections were washed in PBS three times at room temperature and mounted on the glass and dried for 20 min. VECTASHIELD® Antifade Mounting Media (H-1400, Vector Laboratories, USA) was dropped on slides and covered with cover glasses. Images were taken using a confocal microscope (LSM800, ZEISS, Germany) or a fluorescent microscope (BZ-X710, Keyence, Japan).

Statistical analysis

Tukey's multiple comparison test was performed using Prism for the comparison of the mean of the intensity of OXTR binding in the autoradiography experiments.

RESULTS

Generating *Oxtr-ires-Cre* knock-in prairie vole using CRISPR/Cas9

To express *Cre* under the control of *Oxtr* gene expression, we generated *Oxtr-ires-Cre* knock-in prairie vole using CRISPR/Cas9. We designed the knock-in plasmid vector containing *ires-Cre* flanked on either side by 750 bp arms having homology to the target site, with the *ires* place 7 bp downstream of the *Oxtr* stop codon (Fig. 1A). We microinjected crRNA, tracrRNA, and Cas9 protein into fifty four embryos and 23 embryos developed to the 2-cell stage and were transferred into the oviducts of pseudopregnant female voles (the efficiency of development = injected embryos/two-cells, 43.0%). Two candidate pups (cre1 and cre2) were obtained (Birth rate = new borns/transferred embryos, 8.7%) and one (cre1) was confirmed as a knock-in prairie vole by genotyping of tail tissues (Fig. 1B). As further confirmation, the Sanger sequencing around the target region and the inserted sequence showed the knock-in construct was precisely inserted in the target site as planned (Fig. 1B, C) (the efficiency of knock-in = knocked-in voles/newborns, 50%). Based on these results, we concluded that we successfully generated an *Oxtr-ires-Cre* knock-in prairie vole.

Off-target analysis

Results of Sanger sequencing of 14 breeders at the F3 generation showed that a few potential off-target sites had single nucleotide polymorphisms, as to be expected in outbred voles, but no deletions or insertions (indels) indicative of CRISPR editing were detected in any target for any animal (Supplementary Fig. 2). In the analyses of off-target 4, a G/T polymorphism in the PAM sequence was detected in animals #3 and 6, and a G/A polymorphism in the 3′ region adjacent to the PAM sequence was detected in animal #3, 6, and 9, indicated by the red boxes in Fig. S2. In the off-target 5 analyses, an A/C polymorphism outside of the seed sequence in the protospacer sequence was detected in animals #1 and 8. In the analyses of off-target 8, a G/T polymorphism outside of the seed sequence in the protospacer sequence was detected in animal #13. In the analyses of off-target 9, a C/A polymorphism in the protospacer sequence was detected in animal #3, 8, 9, and 13. Such polymorphism in non-coding regions are expected in the outbred vole colony as previously described (Okhovat et al., 2015; King et al., 2016). We conclude that no detectable off-target effects were induced by CRISPR/Cas9 genome editing at the most probable off-target sites in the *Oxtr-ires-Cre* line.

Confirmation of Co-expression of *Oxtr* and *Cre* mRNA

To confirm whether *Cre* co-localizes in cells expressing *Oxtr* in the brain, *Oxtr* and *Cre* mRNA were detected by *in situ* hybridization with RNAscope (Fig. 2; male: +/+, +/Cre, Cre/Cre, each $N = 3$; female: +/+, +/Cre, Cre/Cre, each $N = 3$). In WT brains, *Oxtr* mRNA was detected but no *Cre* mRNA was detected in NAcc. In

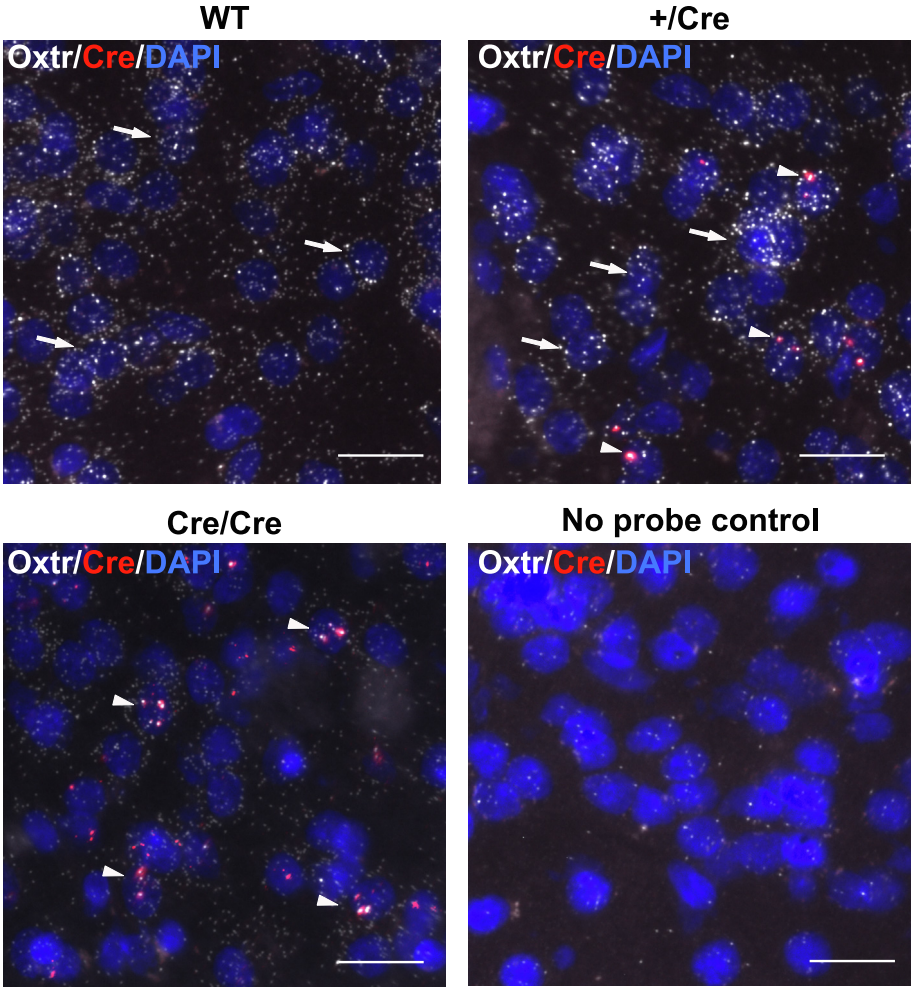

Fig. 2. Co-localization of *Oxtr* and *Cre* mRNA in brains of *Oxtr-ires-Cre* knock-in priaire voles. *Oxtr* and *Cre* mRNA localization in NAcc were analyzed using in situ hybridization with RNAscope in brains of wildtype (WT), heterozygous +/*Cre*, and homozygous *Cre/Cre* prairie voles (male, each $N = 3$; female, each $N = 3$). Note the restriction and co-localization of *Oxtr* and *Cre* signal in aggregates in the Cre/Cre brain.

contrast, *Cre* mRNA was detected in the cells expressing *Oxtr* in NAcc of +/Cre and Cre/Cre animals. Although no probe controls gave us little background noise, the signal with the Cre probe in +/Cre and Cre/Cre brains were much stronger than the background of WT. From these results, we concluded *Cre* mRNAs were transcribed exclusively in *Oxtr*-expressing cells in the brain. Interestingly *Cre* mRNA signal was highly restricted to one or two puncta per cell in +/Cre tissue while *Oxtr* mRNA signal was widely distributed across the cell body. By contrast, in *Cre/Cre* animals, both *Cre* mRNA and *Oxtr* mRNA were both highly restricted and colocalized in their distribution as puncta, suggesting altered processing of *Oxtr-ires-Cre* tandem mRNA produced by the knock-in allele.

Detection of OXTR proteins by autoradiography

The insertion of *ires* sequence is known to affect the expression level of the gene before and after the *ires* sequence (Cheng et al., 2019). We used receptor autoradiography to detect OXTR protein in the brain and analyzed binding density in the NAcc. Quantitative autoradiography showed that OXTR protein levels did not differ between WT and +/Cre (Fig. 3; male: +/+, +/Cre, Cre/Cre, each $N = 3$; female: +/+, +/Cre, Cre/Cre, each $N = 3$). However, OXTR in the brain of Cre/Cre was significantly decreased. These data suggested the insertion of *ires-Cre* sequence significantly reduced expression or translation of the *Oxtr* mRNA. Because of these results, we used heterozygous +/Cre knock-in prairie voles for further experiments.

RETROGRADE TRACING OF *OXTR*-EXPRESSING NEURONS PROJECTING TO NACC

To reveal Oxtr-expressing neurons that project to the NAcc in prairie voles, AAVrg-hSyn-DIO-EGFP was injected into the NAcc of heterozygous +/Cre knock-in prairie voles and the expression of EGFP was mapped in the whole brain (Fig. 4A; male +/Cre, $N = 3$; female +/Cre, $N = 3$). The AAVrg is taken up by terminals in the NAcc and transported back to the nucleus and if *Cre* is present (i.e. only in Oxtr expressing neurons), the neuron will express EGFP. EGFP was detected in anterior olfactory nucleus (AON), prelimbic cortex (PrL), anterior cingulate cortex (Cg2), insular cortex (IC), paraventricular thalamus (PVT), basolateral amygdala, and posteromedial and posterolateral cortical amygdaloid area (PMCo, PLCo) (Fig. 4B–H).

DISCUSSION

Here we report that the first *Oxtr-ires-Cre* knock-in prairie vole was efficiently generated using CRISPR/Cas9 and use Cre-dependent AAVrg to document for the first time several populations of *Oxtr-expressing* neurons that provide direct projections to the prairie vole NAcc. In the prairie vole, we achieved efficient (50%) knock-in of the knock-in plasmid into *Oxtr* gene by using the microinjection of crRNA, tracrRNA, and Cas9 protein, which is consistent with the efficiency showed in the previous report generating knock-in mice (Aida et al., 2015). This technique should be widely applicable for

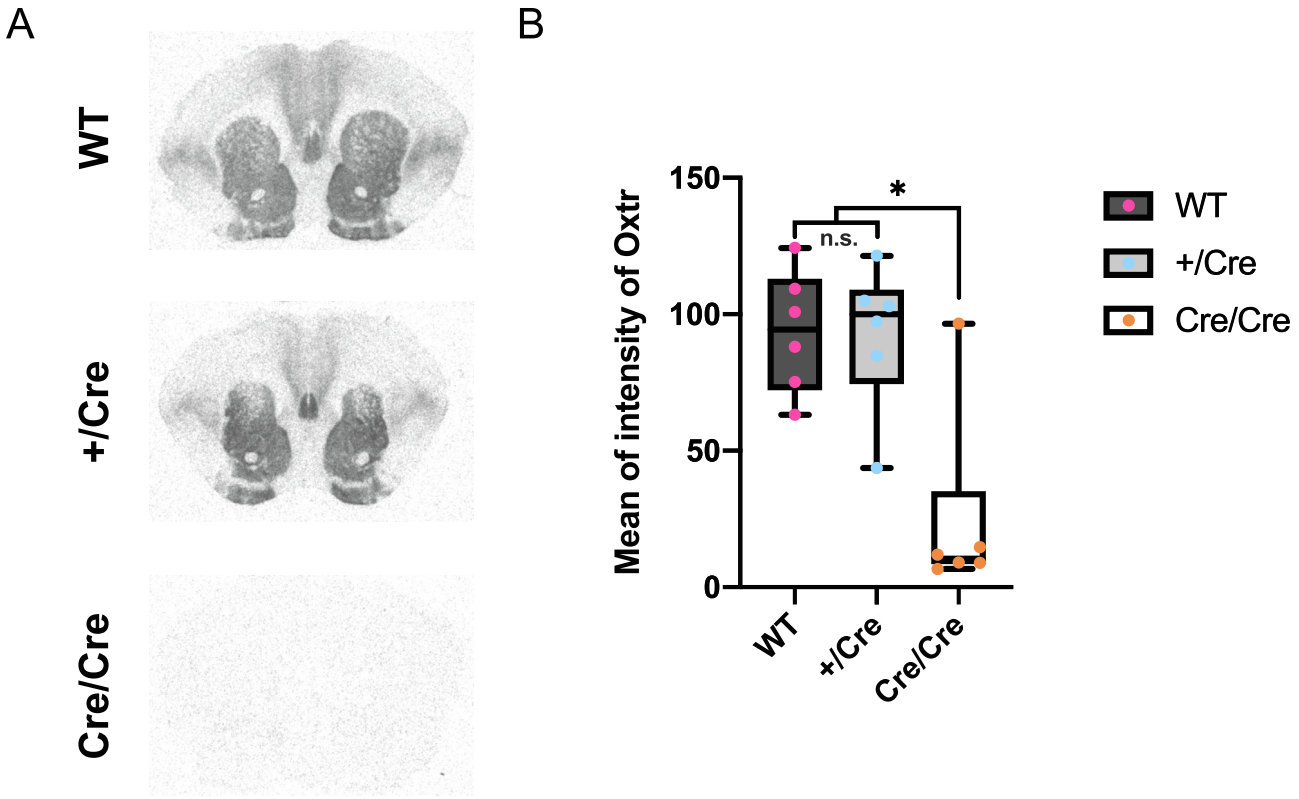

Fig. 3. Detection of OXTR proteins by autoradiography. **(A)** Representative images of autoradiography of brains of WT, heterozygous +/Cre, and homozygous Cre/Cre (male, each $N = 3$; female, each $N = 3$). **(B)** Mean of intensity of Oxtr in NAcc of brains of Cre/Cre was significantly lower than WT and +/Cre (WT, 93.5 ± 9.20; +/Cre, 92.5 ± 10.9; Cre/Cre, 24.6 ± 14.4; WT vs . +/Cre, $P = 0.998$; WT vs. Cre/Cre, $P = 0.0023$; +/Cre vs. Cre/Cre, $P = 0.0026$). The box plot depicts the median and the 25th and 75th quartiles and the whisker shows the 5th and 95th percentile.

generating many mutant lines that can greatly accelerate the elucidation of neural circuit mechanisms underlying social behavior in this model organism.

In previous studies of prairie voles, GFP expressing transgenic voles were generated by lentiviral mediated transgenesis (Donaldson et al., 2009; Keebaugh et al., 2012). Also, prairie vole induced pluripotent cells (iPSCs) have been established by two different groups (Manoli et al., 2012; Katayama et al., 2016). Although those studies suggested the possibility of generating knock-out or knock-in prairie voles using homologous recombination, it was not achieved because of technical difficulties of maintenance of quality of iPSCs and modification of the targeted gene. To overcome the difficulties, we used CRISPR/Cas9 to edit the *Oxtr* gene and successfully generated *Oxtr* knock-out prairie voles in a previous study (Horie et al., 2019). By applying those methods described in the previous paper combined with the high-efficiency method for knocking-in, we successfully generated *Oxtr-ires-Cre* knock-in prairie voles. Sequencing from genome of knock-in prairie voles indicated homologous recombination (HR) was induced in the prairie vole embryos, which means that HR pathway could be conserved in prairie voles.

In the *in situ* hybridization experiments, colocalization of *Oxtr* and *Cre* RNA in the heterozygous and homozygous knock-in prairie voles indicated that the expression of *Cre* is restricted to *Oxtr*-expressing cells. Although *Oxtr* signals in WT brains were detected as sparse, distributed signals, *Cre* mRNA in brains of heterozygous and homozygous knock-in prairie voles seemed to aggregate and signals were more dense than *Oxtr* signals in the WT brains, and *Oxtr* signals also aggregated. These data suggested that the insertion of *Cre* sequence into the *Oxtr* gene might disturb the localization or conformation of *Oxtr* mRNA. Additionally, in the autoradiography experiments, ligand binding was not detected in the homozygous knock-in prairie voles, which suggested the insertion of *Cre* sequence suppressed the translation of OXTR as well. This problem does not appear to be brain specific as a female Cre/Cre animals delivered pups but they did not survive presumably due to starvation because of a defective milk ejection reflex in the mother (The successful rate of weaning (weaned pups/new borns * 100) = 0%), similar to that observe in *Oxtr* KO voles and mice. Although OXTR might not be efficiently translated from the *Cre* inserted allele, there was no difference in the expression of *Oxtr* between WT and heterozygous knock-in voles in autoradiography and CRE-dependent virus expressed well in brains of heterozygous knock-in prairie voles. Those data suggested that heterozygous knock-in prairie voles should be used for further experiments, such as

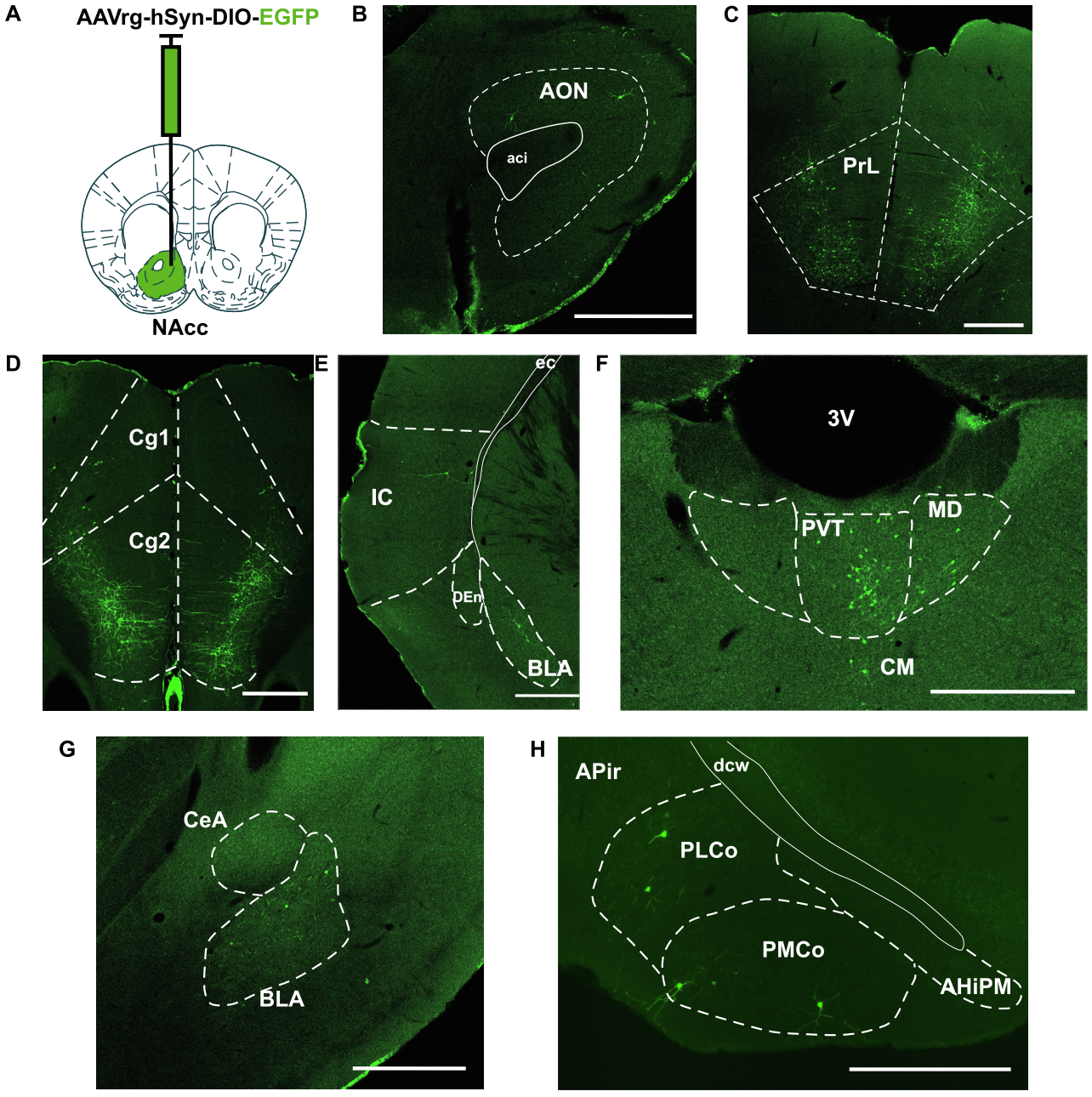

Fig. 4. Retrograde tracing of *Oxtr*-expressing neurons projecting NAcc. **(A)** AAVrg-hSyn-DIO-EGFP was injected into NAcc of *Oxtr-ires-Cre* knock-in prairie voles (male, $N = 3$; female, $N = 3$). **(B–I)** EGFP signals were detected in anterior olfactory nucleus (AON), prelimbic cortex (PrL), anterior cingulate cortex (Cg2), insular cortex (IC), paraventricular thalamus (PVT), basolateral amygdala (BLA), and posteromedial and posterolateral cortical amygdaloid area (PMCo, PLCo). Abbreviations: anterior commissure (aci), anterior cingulate cortex (Cg1), dorsal endopiriform nucleus (DEn), external capsule (ec), 3rd ventricle (3V), mediodorsal thalamic nucleus (MD), central medial thalamic nucleus (CM), central amygdala (CeA), posterior amygdalohippocampal area (AHiPM), amygdalopiriform transition area (APir), deep cerebral white matter (dcw). Scale bar = 500 μm.

chemogenetic or optogenetic manipulation of behaviors, to avoid negative effects of deficits of OXTR proteins to results of behavioral experiments. However, CRE expression may be limited to the highest OXTR expressing neurons due to the abnormal localization of the mRNA. Inserting the *ires-Cre* further downstream of the *Oxtr* stop coding deeper into the 3′ flanking region, or the use of a P2A cleavage sequence might eliminate the aggregation and result in more efficient translation of both the OXTR and CRE.

Neural circuits of *Oxtr*-expressing neurons projecting to NAcc found in the current study are regarded as key components for regulating social cue processing (Walum and Young, 2018). In AON, *Oxtr*-expressing neurons facilitates social recognition by increasing the signal to noise ratio in olfactory bulb (Oettl et al., 2016). Although

the function of *Oxtr*-expressing neurons from AON to NAcc has yet to be reported, this circuit might regulate processing odorant cues of the partner in prairie voles. PrL is a region that has the projection to NAcc, and this circuit enhances females' affiliative behavior during the cohabitation in prairie voles (Amadei et al., 2017). *Oxtr*-expressing neurons in PrL has been proven to regulate the reward processing, social behavior, anxiety, and affiliation behaviors (Young et al., 2001; Sabihi et al., 2014; Everett et al., 2019; He et al., 2019). Combining those findings, we presume that *Oxtr*-expressing neurons in PrL projecting to NAcc may regulate the pair bonding in prairie voles. The BLA has been proposed as a key brain region regulating pair bonding as well (Numan and Young, 2016; Walum and Young, 2018). The BLA to NAcc circuit regulates reward seeking in mice (Ambroggi et al., 2008) and OXT in the amygdala plays a role in regulating social decision-making in non-human primates (Chang et al., 2015). These observations suggest that *Oxtr*-expressing neurons in BLA projecting to NAcc might regulate social reward processing in animals and might facilitate pair bonding in prairie voles. Also, PVT has been emerging as one of the key brain regions regulating the reward processing (Zhu et al., 2016, 2018; Do-Monte et al., 2017). The blockade of OXTR in PVT decreased maternal crouching behavior toward pups in mice (Watarai et al., 2020). Although the function of PVT in regulating social behaviors has yet to be investigated, these findings and the projection that was found in the current study suggested that *Oxtr*-expressing neurons in PVT projecting to NAcc might regulate the pair bonding behavior in prairie voles, and their role should be investigated in future studies.

A previous mouse study showed that NAcc core had afferent inputs of *Oxtr*-expressing neurons from PVN, AON, PVT, BLA, central amygdala (CeA), cortical amygdala (CoA), ventral tegmental area (VTA), dorsal raphe nucleus (dRph), ventral subiculum, and ventral hippocampal CA1 (vCA1) by combining the immunostaining of *Oxtr-Venus* knock-in mice (Yoshida et al., 2009) and the retrograde tracing from NAcc core by rabies virus (RBV) carrying tdTomato (Dolen et al., 2013). Another paper showed that *Oxtr*-expressing neurons in VTA had projections to NAcc in mice by the injection of CRE-dependent AAV-chanelrhodopsin2 (ChR2) into VTA of *Oxtr-Cre* transgenic mice (Peris et al., 2017). By the injection of CRE-dependent AAV-ChR2 into PFC of *Oxtr-Cre* transgenic mice, the projection of *Oxtr*-expressing neurons from PFC to NAcc were shown as well (Tan et al., 2019). Thus, we detected a more limited distribution of *Oxtr*-expressing neurons projecting to the NAcc, which suggests that due to the reduced expression/translation of the *Oxtr-ires-Cre* transcript, we may only be detecting the neurons with the most robust *Oxtr* expression. However, we did detect one set of *Oxtr* neurons with robust signal that was not detected in mice, the ACC. Although we targeted the entire NAcc and didn't distinguish between core and shell, we found that *Oxtr*-expressing neurons in ACC had projections to NAcc in prairie voles, which was not found in previous studies of mice (Dolen et al., 2013). In prairie voles, inhibition of OXTR in ACC impaired consolation behaviors toward the stressed partners in prairie voles (Burkett et al., 2016). Based on these studies, we propose the hypothesis that *Oxtr*-expressing neurons from ACC to NAcc found in the current study might be a prairie vole specific circuit that regulates partner specific affiliation or consolation behaviors that is not present in mice. Although further confirmation to make sure the specificity of the neural circuits of *Oxtr*-expressing neurons between NAcc core and shell are required, this circuit was recognized only in prairie voles, not in mice and rats.

Regarding IC, although the circuit of *Oxtr*-expressing neurons from IC to NAcc was not confirmed in mice, we found it in prairie voles, but there were only a few labeled neurons in IC of prairie voles (Fig. 4E). IC to NAcc circuits have been regarded as the key brain region that regulates social approach behaviors to the stressed juvenile in rats (Rogers-Carter et al., 2019). Blockade of OXTR in IC disrupted social approach behaviors in rats (Rogers-Carter et al., 2018). Based on these studies, we hypothesis that rats and prairie vole share a common circuit of *Oxtr*-expressing neurons from IC projecting to NAcc which is absent in mice. *Oxtr*-expressing neurons in vCA1 projecting to NAcc were not found in brains of prairie voles. The vCA1 to NAcc circuit is known as a region storing social memory in mice (Okuyama et al., 2016). In PVN, CeA, VTA, and dRph of prairie voles, outputs of *Oxtr*-expressing neurons to NAcc were not detected. Due to the altered mRNA localization and translation of the *Oxtr-ires-Cre* mRNA, we cannot be confident that a lack of signal in our study is strong evidence of a lack of connectivity in prairie voles. Alternate strategies of generating *Oxtr-cre* prairie voles are needed to have confidence of the absence of *Oxtr*-neuron connections with NAcc in vCA1, VTA, dRph and other regions.

These differences of projections between mice, rats, and prairie voles might come from differences in neurotropism between the two retrograde viruses used for the retrograde tracing (Sun et al., 2019). For further comparison, *Oxtr-ires-Cre voles* should be injected with CRE-dependent RBV and the projections must be compared with the current data in the future study. Also, the lower level of the expression of *Cre* because of the aggregation of *Cre* mRNA might affect results of retrograde tracing. RNAscope experiments showed that *Cre* containing RNAs aggregated, which means translation of *Cre* RNA might be suppressed. Also we were not able to detect CRE proteins in fixed brain slices by immunostaining with anti-CRE antibodies (data not shown). From those data, we presumed that it was difficult to detect CRE-dependent EGFP in some brain regions that express less *Oxtr*. Because of these limitations, our analysis was limited to a qualitative description in adults and we were not able to reliably determine whether there are sex differences or developmental changes in *Oxtr* neurons projecting to the NAcc in the current study.

Oxtr-ires-Cre knock-in prairie voles generated in the current study is the first knock-in prairie vole that is an unprecedented tool to investigate Oxtr-expressing neural circuits related to the regulation of social affiliation, albeit with unfortunate limitations. Combining

Oxtr-ires-Cre knock-in prairie voles with using CRE-dependent hM3Dq/hM4Di expression, or ChR2/halorhodopsin enable researchers to manipulate *Oxtr*-expressing neural circuits during partner preference tests (Boender and Young, 2020). It will be possible to monitor the activity of *Oxtr*-expressing neurons using CRE-dependent GCaMP *in vivo* as well. We believe that those future experiments using *Oxtr-ire-Cre* knock-in voles will greatly accelerate our elucidation of the neural circuit mechanisms underlying social bonding.

ACKNOWLEDGEMENTS

We thank Lorra Julian for help maintaining the vole colony at Emory. The research performed in Japan was funded by the Strategic Research Program for Brain Sciences from Japan Agency for Medical Research and Development (AMED; 18dm0107076h0003, 2016–2020) and JSPS Grant-in-Aid for Scientific Research (15H02442, 2015–2018) to KN, and Grant-in-Aid for JSPS Fellows (16J05070, 2016–019) to KH. The work performed at Emory in the USA was supported by NIH grants R01MH112788 and P50MH100023 to LJY and P51OD11132 to YNPRC.

REFERENCES

Aida T, Chiyo K, Usami T, Ishikubo H, Imahashi R, Wada Y, Tanaka KF, Sakuma T, et al. (2015) Cloning-free CRISPR/Cas system facilitates functional cassette knock-in in mice. Genome Biol 16:87.

Amadei EA, Johnson ZV, Jun Kwon Y, Shpiner AC, Saravanan V, Mays WD, Ryan SJ, Walum H, et al. (2017) Dynamic corticostriatal activity biases social bonding in monogamous female prairie voles. Nature 546:297–301.

Ambroggi F, Ishikawa A, Fields HL, Nicola SM (2008) Basolateral amygdala neurons facilitate reward-seeking behavior by exciting nucleus accumbens neurons. Neuron 59:648–661.

Aragona BJ, Liu Y, Yu YJ, Curtis JT, Detwiler JM, Insel TR, Wang Z (2006) Nucleus accumbens dopamine differentially mediates the formation and maintenance of monogamous pair bonds. Nat Neurosci 9:133–139.

Arai A, Hirota Y, Miyase N, Miyata S, Young LJ, Osako Y, Yuri K, Mitsui S (2016) A single prolonged stress paradigm produces enduring impairments in social bonding in monogamous prairie voles. Behav Brain Res 315:83–93.

Barrangou R, Fremaux C, Deveau H, Richards M, Boyaval P, Moineau S, Romero DA, Horvath P (2007) CRISPR provides acquired resistance against viruses in prokaryotes. Science 315:1709–1712.

Barrett CE, Arambula SE, Young LJ (2015) The oxytocin system promotes resilience to the effects of neonatal isolation on adult social attachment in female prairie voles. Transl Psychiatry 5 e606.

Boender AJ, Young LJ (2020) Oxytocin, vasopressin and social behavior in the age of genome editing: A comparative perspective. Horm Behav 124 104780.

Bosch OJ, Dabrowska J, Modi ME, Johnson ZV, Keebaugh AC, Barrett CE, Ahern TH, Guo J, et al. (2016) Oxytocin in the nucleus accumbens shell reverses CRFR2-evoked passive stress-coping after partner loss in monogamous male prairie voles. Psychoneuroendocrinology 64:66–78.

Bosch OJ, Young LJ (2018) Oxytocin and social relationships: from attachment to bond disruption. Curr Top Behav Neurosci 35:97–117.

Burkett JP, Andari E, Johnson ZV, Curry DC, de Waal FB, Young LJ (2016) Oxytocin-dependent consolation behavior in rodents. Science 351:375–378.

Chamberlin NL, Du B, de Lacalle S, Saper CB (1998) Recombinant adeno-associated virus vector: use for transgene expression and anterograde tract tracing in the CNS. Brain Res 793:169–175.

Chang SW, Fagan NA, Toda K, Utevsky AV, Pearson JM, Platt ML (2015) Neural mechanisms of social decision-making in the primate amygdala. Proc Natl Acad Sci U S A 112:16012–16017.

Cheng AH, Fung SW, Cheng HM (2019) Limitations of the Avp-IRES2-Cre (JAX #023530) and Vip-IRES-Cre (JAX #010908) models for chronobiological investigations. J Biol Rhythms 34:634–644.

Cho SW, Kim S, Kim JM, Kim JS (2013) Targeted genome engineering in human cells with the Cas9 RNA-guided endonuclease. Nat Biotechnol 31:230–232.

Choe HK, Reed MD, Benavidez N, Montgomery D, Soares N, Yim YS, Choi GB (2015) Oxytocin mediates entrainment of sensory stimuli to social cues of opposing valence. Neuron 87:152–163.

Cong L, Ran FA, Cox D, Lin S, Barretto R, Habib N, Hsu PD, Wu X, et al. (2013) Multiplex genome engineering using CRISPR/Cas systems. Science 339:819–823.

Deltcheva E, Chylinski K, Sharma CM, Gonzales K, Chao Y, Pirzada ZA, Eckert MR, Vogel J, et al. (2011) CRISPR RNA maturation by trans-encoded small RNA and host factor RNase III. Nature 471:602–607.

Do-Monte FH, Minier-Toribio A, Quinones-Laracuente K, Medina-Colon EM, Quirk GJ (2017) Thalamic regulation of sucrose seeking during unexpected reward omission. Neuron 94. 388–400 e384.

Dolen G, Darvishzadeh A, Huang KW, Malenka RC (2013) Social reward requires coordinated activity of nucleus accumbens oxytocin and serotonin. Nature 501:179–184.

Donaldson ZR, Yang SH, Chan AW, Young LJ (2009) Production of germline transgenic prairie voles (Microtus ochrogaster) using lentiviral vectors. Biol Reprod 81:1189–1195.

Donaldson ZR, Young LJ (2008) Oxytocin, vasopressin, and the neurogenetics of sociality. Science 322:900–904.

Everett N, Baracz S, Cornish J (2019) Oxytocin treatment in the prelimbic cortex reduces relapse to methamphetamine-seeking and is associated with reduced activity in the rostral nucleus accumbens core. Pharmacol Biochem Behav 183:64–71.

Feldman R (2012) Oxytocin and social affiliation in humans. Horm Behav 61:380–391.

Gobrogge KL, Liu Y, Young LJ, Wang Z (2009) Anterior hypothalamic vasopressin regulates pair-bonding and drug-induced aggression in a monogamous rodent. Proc Natl Acad Sci U S A 106:19144–19149.

He Z, Young L, Ma XM, Guo Q, Wang L, Yang Y, Luo L, Yuan W, et al. (2019) Increased anxiety and decreased sociability induced by paternal deprivation involve the PVN-PrL OTergic pathway. Elife 8.

Hidema S, Fukuda T, Hiraoka Y, Mizukami H, Hayashi R, Otsuka A, Suzuki S, Miyazaki S, et al. (2016) Generation of Oxtr cDNA(HA)-Ires-Cre mice for gene expression in an oxytocin receptor specific manner. J Cell Biochem 117:1099–1111.

Hirota Y, Arai A, Young LJ, Osako Y, Yuri K, Mitsui S (2020) Oxytocin receptor antagonist reverses the blunting effect of pair bonding on fear learning in monogamous prairie voles. Horm Behav 120 104685.

Horie K, Hidema S, Hirayama T, Nishimori K (2015) In vitro culture and in vitro fertilization techniques for prairie voles (Microtus ochrogaster). Biochem Biophys Res Commun 463:907–911.

Horie K, Inoue K, Suzuki S, Adachi S, Yada S, Hirayama T, Hidema S, Young LJ, et al. (2019) Oxytocin receptor knockout prairie voles generated by CRISPR/Cas9 editing show reduced preference for social novelty and exaggerated repetitive behaviors. Horm Behav 111:60–69.

Insel TR, Shapiro LE (1992) Oxytocin receptor distribution reflects social organization in monogamous and polygamous voles. Proc Natl Acad Sci U S A 89:5981–5985.

Johnson ZV, Walum H, Jamal YA, Xiao Y, Keebaugh AC, Inoue K, Young LJ (2016) Central oxytocin receptors mediate mating-induced partner preferences and enhance correlated activation across forebrain nuclei in male prairie voles. Horm Behav 79:8–17.
Johnson ZV, Walum H, Xiao Y, Riefkohl PC, Young LJ (2017) Oxytocin receptors modulate a social salience neural network in male prairie voles. Horm Behav 87:16–24.
Johnson ZV, Young LJ (2015) Neurobiological mechanisms of social attachment and pair bonding. Curr Opin Behav Sci 3:38–44.
Johnson ZV, Young LJ (2017) Oxytocin and vasopressin neural networks: Implications for social behavioral diversity and translational neuroscience. Neurosci Biobehav Rev 76:87–98.
Jurek B, Neumann ID (2018) The oxytocin receptor: from intracellular signaling to behavior. Physiol Rev 98:1805–1908.
Katayama M, Hirayama T, Horie K, Kiyono T, Donai K, Takeda S, Nishimori K, Fukuda T (2016) Induced pluripotent stem cells with six reprogramming factors from prairie vole, which is an animal model for social behaviors. Cell Transplant 25:783–796.
Keebaugh AC, Barrett CE, Laprairie JL, Jenkins JJ, Young LJ (2015) RNAi knockdown of oxytocin receptor in the nucleus accumbens inhibits social attachment and parental care in monogamous female prairie voles. Soc Neurosci 10:561–570.
Keebaugh AC, Modi ME, Barrett CE, Jin C, Young LJ (2012) Identification of variables contributing to superovulation efficiency for production of transgenic prairie voles (Microtus ochrogaster). Reprod Biol Endocrinol 10:54.
King LB, Walum H, Inoue K, Eyrich NW, Young LJ (2016) Variation in the oxytocin receptor gene predicts brain region-specific expression and social attachment. Biol Psychiatry 80:160–169.
Knobloch HS, Charlet A, Hoffmann LC, Eliava M, Khrulev S, Cetin AH, Osten P, Schwarz MK, et al. (2012) Evoked axonal oxytocin release in the central amygdala attenuates fear response. Neuron 73:553–566.
Lafferty CK, Yang AK, Mendoza JA, Britt JP (2020) Nucleus accumbens cell type- and input-specific suppression of unproductive reward seeking. Cell Rep 30. 3729–3742 e3723.
Mali P, Yang L, Esvelt KM, Aach J, Guell M, DiCarlo JE, Norville JE, Church GM (2013) RNA-guided human genome engineering via Cas9. Science 339:823–826.
Manoli DS, Subramanyam D, Carey C, Sudin E, Van Westerhuyzen JA, Bales KL, Blelloch R, Shah NM (2012) Generation of induced pluripotent stem cells from the prairie vole. PLoS ONE 7 e38119.
Marlin BJ, Mitre M, D'Amour JA, Chao MV, Froemke RC (2015) Oxytocin enables maternal behaviour by balancing cortical inhibition. Nature 520:499–504.
McGraw LA, Young LJ (2010) The prairie vole: an emerging model organism for understanding the social brain. Trends Neurosci 33:103–109.
Modi ME, Inoue K, Barrett CE, Kittelberger KA, Smith DG, Landgraf R, Young LJ (2015) Melanocortin receptor agonists facilitate oxytocin-dependent partner preference formation in the prairie vole. Neuropsychopharmacology 40:1856–1865.
Numan M, Young LJ (2016) Neural mechanisms of mother-infant bonding and pair bonding: similarities, differences, and broader implications. Horm Behav 77:98–112.
Oettl LL, Ravi N, Schneider M, Scheller MF, Schneider P, Mitre M, da Silva GM, Froemke RC, et al. (2016) Oxytocin enhances social recognition by modulating cortical control of early olfactory processing. Neuron 90:609–621.
Okhovat M, Berrio A, Wallace G, Ophir AG, Phelps SM (2015) Sexual fidelity trade-offs promote regulatory variation in the prairie vole brain. Science 350:1371–1374.
Okuyama T, Kitamura T, Roy DS, Itohara S, Tonegawa S (2016) Ventral CA1 neurons store social memory. Science 353:1536–1541.
Otis JM, Zhu M, Namboodiri VMK, Cook CA, Kosyk O, Matan AM, Ying R, Hashikawa Y, et al. (2019) Paraventricular thalamus projection neurons integrate cortical and hypothalamic signals for cue-reward processing. Neuron 103(423–431) e424.
Peris J, MacFadyen K, Smith JA, de Kloet AD, Wang L, Krause EG (2017) Oxytocin receptors are expressed on dopamine and glutamate neurons in the mouse ventral tegmental area that project to nucleus accumbens and other mesolimbic targets. J Comp Neurol 525:1094–1108.
Pohl TT, Young LJ, Bosch OJ (2019) Lost connections: oxytocin and the neural, physiological, and behavioral consequences of disrupted relationships. Int J Psychophysiol 136:54–63.
Rogers CN, Ross AP, Sahu SP, Siegel ER, Dooyema JM, Cree MA, Stopa EG, Young LJ, et al. (2018) Oxytocin- and arginine vasopressin-containing fibers in the cortex of humans, chimpanzees, and rhesus macaques. Am J Primatol 80 e22875.
Rogers-Carter MM, Djerdjaj A, Gribbons KB, Varela JA, Christianson JP (2019) Insular cortex Projections to Nucleus Accumbens Core Mediate Social Approach to Stressed Juvenile Rats. J Neurosci 39:8717–8729.
Rogers-Carter MM, Varela JA, Gribbons KB, Pierce AF, McGoey MT, Ritchey M, Christianson JP (2018) Insular cortex mediates approach and avoidance responses to social affective stimuli. Nat Neurosci 21:404–414.
Ross HE, Cole CD, Smith Y, Neumann ID, Landgraf R, Murphy AZ, Young LJ (2009) Characterization of the oxytocin system regulating affiliative behavior in female prairie voles. Neuroscience 162:892–903.
Sabihi S, Durosko NE, Dong SM, Leuner B (2014) Oxytocin in the prelimbic medial prefrontal cortex reduces anxiety-like behavior in female and male rats. Psychoneuroendocrinology 45:31–42.
Smith AS, Wang Z (2014) Hypothalamic oxytocin mediates social buffering of the stress response. Biol Psychiatry 76:281–288.
Sun L, Tang Y, Yan K, Yu J, Zou Y, Xu W, Xiao K, Zhang Z, et al. (2019) Differences in neurotropism and neurotoxicity among retrograde viral tracers. Mol Neurodegener 14:8.
Tan Y, Singhal SM, Harden SW, Cahill KM, Nguyen DM, Colon-Perez LM, Sahagian TJ, Thinschmidt JS, et al. (2019) Oxytocin receptors are expressed by glutamatergic prefrontal cortical neurons that selectively modulate social recognition. J Neurosci 39:3249–3263.
Tervo DG, Hwang BY, Viswanathan S, Gaj T, Lavzin M, Ritola KD, Lindo S, Michael S, et al. (2016) A designer AAV variant permits efficient retrograde access to projection neurons. Neuron 92:372–382.
Walum H, Young LJ (2018) The neural mechanisms and circuitry of the pair bond. Nat Rev Neurosci 19:643–654.
Wang H, Yang H, Shivalila CS, Dawlaty MM, Cheng AW, Zhang F, Jaenisch R (2013) One-step generation of mice carrying mutations in multiple genes by CRISPR/Cas-mediated genome engineering. Cell 153:910–918.
Watarai A, Tsutaki S, Nishimori K, Okuyama T, Mogi K, Kikusui T (2020) The blockade of oxytocin receptors in the paraventricular thalamus reduces maternal crouching behavior over pups in lactating mice. Neurosci Lett 720 134761.
Wei D, Lee D, Cox CD, Karsten CA, Penagarikano O, Geschwind DH, Gall CM, Piomelli D (2015) Endocannabinoid signaling mediates oxytocin-driven social reward. Proc Natl Acad Sci U S A 112:14084–14089.
Wiedenheft B, Sternberg SH, Doudna JA (2012) RNA-guided genetic silencing systems in bacteria and archaea. Nature 482:331–338.
Witt DM, Carter CS, Lnsel TR (1991) Oxytocin receptor binding in female prairie voles: endogenous and exogenous oestradiol stimulation. J Neuroendocrinol 3:155–161.
Yokoi S, Naruse K, Kamei Y, Ansai S, Kinoshita M, Mito M, Iwasaki S, Inoue S, et al. (2020) Sexually dimorphic role of oxytocin in medaka mate choice. Proc Natl Acad Sci U S A 117: 4802–4808.
Yoshida M, Takayanagi Y, Inoue K, Kimura T, Young LJ, Onaka T, Nishimori K (2009) Evidence that oxytocin exerts anxiolytic effects via oxytocin receptor expressed in serotonergic neurons in mice. J Neurosci 29:2259–2271.

Young KA, Gobrogge KL, Liu Y, Wang Z (2011) The neurobiology of pair bonding: insights from a socially monogamous rodent. Front Neuroendocrinol 32:53–69.
Young LJ, Lim MM, Gingrich B, Insel TR (2001) Cellular mechanisms of social attachment. Horm Behav 40:133–138.
Young LJ, Wang Z (2004) The neurobiology of pair bonding. Nat Neurosci 7:1048–1054.
Zhu Y, Nachtrab G, Keyes PC, Allen WE, Luo L, Chen X (2018) Dynamic salience processing in paraventricular thalamus gates associative learning. Science 362:423–429.
Zhu Y, Wienecke CF, Nachtrab G, Chen X (2016) A thalamic input to the nucleus accumbens mediates opiate dependence. Nature 530:219–222.

APPENDIX A. SUPPLEMENTARY DATA

Supplementary data to this article can be found online at https://doi.org/10.1016/j.neuroscience.2020.08.023.

(Received 2 July 2020, Accepted 17 August 2020)